

Switching of the magnetic order in $\text{CeRhIn}_{5-x}\text{Sn}_x$ in the vicinity of its quantum critical point

S. Raymond,^{1,2} J. Buhot*,^{1,2} E. Ressouche,^{1,2} F. Bourdarot,^{1,2} G. Knebel,^{1,2} and G. Lapertot^{1,2}

¹*Univ. Grenoble Alpes, INAC-SPSMS, F-38000 Grenoble, France*

²*CEA, INAC-SPSMS, F-38000 Grenoble, France*

(Dated: March 1, 2022)

We report neutron diffraction experiments performed in the tetragonal antiferromagnetic heavy fermion system $\text{CeRhIn}_{5-x}\text{Sn}_x$ in its (x, T) phase diagram up to the vicinity of the critical concentration $x_c \approx 0.40$, where long range magnetic order is suppressed. The propagation vector of the magnetic structure is found to be $\mathbf{k}_{\text{IC}}=(1/2, 1/2, k_l)$ with k_l increasing from $k_l=0.298$ to $k_l=0.410$ when x increases from $x=0$ to $x=0.26$. Surprisingly, for $x=0.30$, the order has changed drastically and a commensurate antiferromagnetism with $\mathbf{k}_{\text{C}}=(1/2, 1/2, 0)$ is found. This concentration is located in the proximity of the quantum critical point where superconductivity is expected.

PACS numbers:

The interplay between magnetism and superconductivity is one of the most studied topics in the physics of strongly correlated electron systems. The occurrence of competing or coexisting antiferromagnetic and superconducting ground states is common to many systems: high- T_c cuprates, new iron-based superconductors and heavy fermion (HF) compounds [1]. In this context, the family of HF compounds CeMIn_5 ($M = \text{Co}, \text{Rh}, \text{Ir}$), the so-called 1-1-5 compounds, is a fabulous playground since the chemical substitution, the application of pressure or magnetic field lead to the possibility to tune the Néel temperature T_N and the superconducting transition temperature T_c to different levels with either $T_N \geq T_c$ or $T_N \leq T_c$ [2, 3]. The parent compound CeRhIn_5 crystallizes in the tetragonal space group $P4/\text{mmm}$. It orders magnetically in an incommensurate helicoidal structure below 3.8 K at ambient pressure. Pressure induced superconductivity occurs above 1 GPa and at around 2 GPa, the Néel temperature equals the superconducting transition temperature. At higher pressure antiferromagnetism is superseded by a pure superconducting state. However a magnetic field, applied in the basal plane of the tetragonal structure, inside this superconducting phase, restores an antiferromagnetic order. This phase exists even far above the superconducting upper critical field H_{c2} [4, 5]. Such a field induced antiferromagnetism bears similarity to the one observed in CeCoIn_5 out of the purely d -wave superconducting state, although in this latter case, the magnetic order disappears at H_{c2} [6].

Microscopic informations on the magnetic structures are essential in order to grasp the different ingredients at play. In CeRhIn_5 , this is provided essentially by NQR [7] since the triple conditions of high magnetic field, high

pressure and low temperature preclude to perform neutron diffraction experiments, which were carried out either under pressure [8, 9] or under magnetic field [10]. Another possible route is to substitute Sn for In, which acts as a positive pressure in the phase diagram. This substitution corresponds to electron doping. In $\text{CeRhIn}_{5-x}\text{Sn}_x$, a quantum critical point occurs for $x_c \approx 0.40$ [11–13] and pressure induced superconductivity is reported in $\text{CeRhIn}_{4.84}\text{Sn}_{0.16}$ above 0.8 GPa with however a reduced maximum value of T_c [14]. In the present work, we determine the evolution of the magnetic structure as a function of x in $\text{CeRhIn}_{5-x}\text{Sn}_x$.

Single crystals of $\text{CeRhIn}_{5-x}\text{Sn}_x$ were grown by the self flux method [15] starting with a ratio $\text{Ce} : \text{Rh} : \text{In} : \text{Sn} = 1 : 1 : 20 : y$. In Ref.[11], a linear relationship between the actual Sn concentration, x , in the crystal and the starting Sn ratio y in the flux has been found with $x=0.4y$. The same relation in the determination of the actual concentration is taken throughout this article since bulk measurements performed on samples of the same batch of the one for the neutron diffraction experiments, which preliminary report can be found in Ref. [16], indicate consistent values of T_N with the study of Bauer et al. [11]. Rectangular-shaped samples were cut for neutron scattering experiment for $x=0.10, 0.16, 0.20, 0.26$ and 0.30 with dimensions given in Table I.

The measurements were performed on the two-

TABLE I: Experimental conditions. The sample size is given along the a , b and c -axis directions (in this order).

x	Sample size (mm^3)	Sample Environnement
0.10	$2 \times 2 \times 1$	^4He cryostat
0.16	$2.1 \times 1.3 \times 1.8$	^3He cryostat
0.20	$2 \times 2 \times 1$	^3He cryostat
0.26	$2 \times 2 \times 2$	^3He and ^3He - ^4He dilution cryostat
0.30	$3 \times 3 \times 1$	^3He - ^4He dilution cryostat

*Present Address : Laboratoire Matériaux et Phénomènes Quantiques, UMR 7162 CNRS, Université Paris Diderot, 75205 Paris, France.

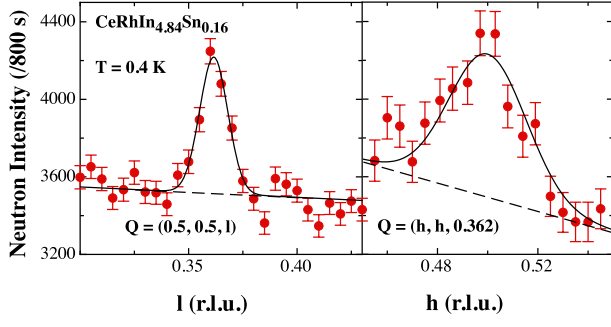


FIG. 1: \mathbf{Q} -scans performed along the $[0,0,1]$ and $[1,1,0]$ directions for $\text{CeRhIn}_{4.84}\text{Sn}_{0.16}$ at $T=0.4$ K. The full lines are Gaussian fits and the dash lines indicate the background.

axis D23-CEA-CRG (Collaborating Research Group) thermal-neutron diffractometer equipped with a lifting detector at the Institut Laue Langevin, Grenoble. A copper monochromator provides an unpolarized beam with a wavelength of $\lambda = 1.283$ Å. The samples were mounted in different kinds of cryostats accordingly to their respective Néel temperatures (See Table I). The $[1, -1, 0]$ direction was set as the vertical axis. For each sample, crystal and magnetic structures were refined and details of the method are given in a previous study performed on CeRhIn_5 [10]. The additional parameters compared to CeRhIn_5 are the occupations of the two inequivalent In sites by Sn substituent (In(1) in the Ce-plane and In(2) in between these planes). A previous crystallographic study performed using a neutron four circle diffractometer on $x=0.16$ suggests that Sn preferentially occupies the In(1) site (66 %) compared to the In(2) site (34 %) [16]. Similar conclusion is drawn from the NQR results obtained for $x=0.044$ [17]. In the present study, it is not possible to discuss this point. However this does not affect the results on the magnetic structure determination.

For each concentration, the search for the magnetic propagation vector was made by doing wide scans along $\mathbf{Q}=(1/2, 1/2, l)$. In this paper, the scattering vector, \mathbf{Q} , is written as $\mathbf{Q}=\boldsymbol{\tau}+\mathbf{q}$ where $\boldsymbol{\tau}$ is a Brillouin zone center and $\mathbf{q}=(h, k, l)$. All coordinates are expressed in reciprocal lattice units (r.l.u.). All the raw data shown in the figures of the paper were collected in the first Brillouin zone where $\mathbf{Q}=\mathbf{q}$. Representative \mathbf{Q} -scans measured for $x=0.16$ along $[0,0,1]$ and $[1,1,0]$ directions at $T=0.4$ K are shown in Figure 1. Figure 2 shows similar scans performed along $\mathbf{Q}=(1/2, 1/2, l)$ with normalized intensities for $x=0.10, 0.26$ and 0.30 for temperatures below and above the respective T_N of each sample. These data show the smooth evolution of the c -axis component of the propagation vector between $x=0.10$ and $x=0.26$. For $x=0.30$, the magnetic peak position becomes commensurate with a zero c -axis component. It was also checked for each x , that a unique propagation vector exists. This is shown in Fig. 2 for $x=0.26$, where no commensurate

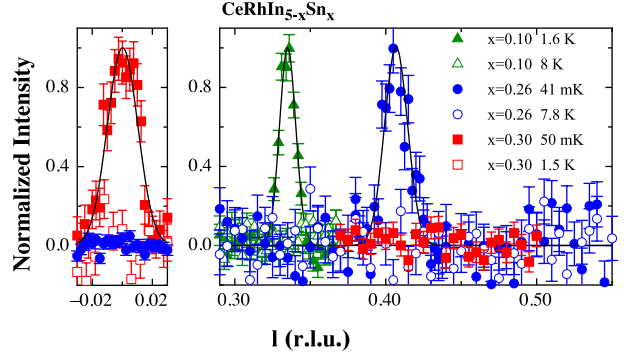


FIG. 2: \mathbf{Q} -scans performed along the $[0,0,1]$ direction for $x=0.10, 0.26$ and 0.30 for temperatures below and above their respective Néel temperatures. The full lines are Gaussian fits.

signal is evidenced (full circles) and for $x=0.30$ where no incommensurate signal exists (full square). The main result of this paper is the evidence for a switching of incommensurate magnetic order with $\mathbf{k}_{\text{IC}}=(1/2, 1/2, k_l)$ ($0.298 \leq k_l \leq 0.410$) to commensurate magnetic order with $\mathbf{k}_{\text{C}}=(1/2, 1/2, 0)$ (so-called C-type magnetic structure) in $\text{CeRhIn}_{5-x}\text{Sn}_x$ above $x=0.26$.

Figure 3 shows the temperature dependence of a \mathbf{Q} -scan performed along $[0,0,1]$ for $x=0.20$. The c -axis value of the propagation vector, k_l , does not change significantly with temperature although we cannot exclude a small shift to a lower value in the vicinity of T_N . The temperature dependence of the order parameter (proportional to the square root of the background subtracted neutron intensity, I) was therefore measured on the maximum of the Bragg peak position for each concentration. Normalized intensities (I/I_0) are shown in Figure 4. The Néel temperature given in Table II is obtained from a phenomenological description of these curves with $I/I_0 \propto 1 - (T/T_N)^\alpha$ with α a free parameter. The weakness of the signal does not allow to distinguish between Bragg and diffuse scattering in the vicinity of the phase transition. The best fit is obtained with $\alpha \approx 0.6$ for $x=0.10, 0.16, 0.20$ and $\alpha \approx 0.2$ for $x=0.26, 0.30$. This change of behavior could originate from different intrinsic magnetic properties near x_c , different distributions of concentra-

TABLE II: Experimental results for the propagation vector \mathbf{k} , the Néel temperature, T_N , and the ordered moment M_0 .

x	\mathbf{k}	$T_N(\text{K})$	$M_0 (\mu_B)$
0	(0.5, 0.5, 0.298)	3.80 (1)	0.59 (2)
0.10	(0.5, 0.5, 0.335)	3.30 (2)	0.58 (2)
0.16	(0.5, 0.5, 0.362)	2.73 (3)	0.49 (2)
0.20	(0.5, 0.5, 0.389)	2.03 (3)	0.59 (4)
0.26	(0.5, 0.5, 0.410)	1.54 (9)	0.28 (2)
0.30	(0.5, 0.5, 0)	0.84 (3)	0.25 (2)

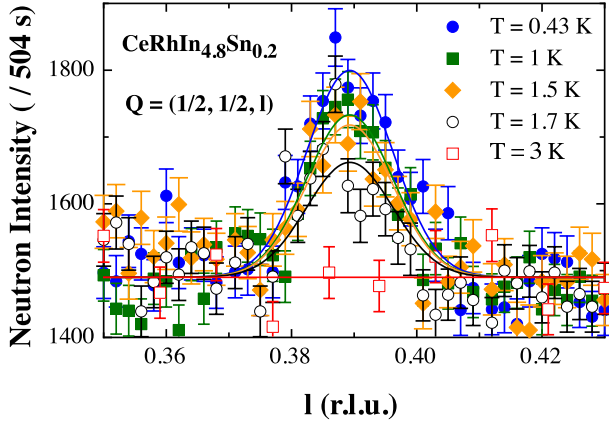


FIG. 3: Temperature dependence of a \mathbf{Q} -scan performed along $[0,0,1]$ for $x=0.20$. Lines are Gaussian fits.

tion or it could be an artifact of this phenomenological method used to determine the Néel temperature. The T_N values obtained are compatible with the one reported by bulk measurements, having in mind that the determinations from specific heat and resistive anomalies show also some differences among themselves [11–14].

Similarly to CeRhIn_5 [10], the magnetic moment was calculated assuming an helicoidal structure up to $x=0.26$. For $x=0.30$, the commensurate propagation vector implies a collinear structure. The ordered moments are assumed to be in the basal plane of the tetragonal structure as for the pure compound [10]. Consequently for $x=0.30$, two magnetic domains corresponding to two orthogonal directions of magnetic moments are considered (an equal domain population is assumed). The values of the propagation vector, \mathbf{k} , the Néel temperature, T_N , and the ordered moment, M_0 , are summarized in Table II and in Figure 5. The variation of the Néel temperature with x is smooth and agrees with bulk measurements. The magnetic moment evolves only slightly up to $x=0.20$ and then decreases significantly. The c -axis component of the propagation vector increases linearly with x up to $x=0.26$, following $k_l(x)=0.295(4)+0.44(2)\times x$. For $x=0.30$, the propagation vector has switched to $\mathbf{k}_C=(1/2, 1/2, 0)$. The lines drawn for $T_N(x)$ and $M_0(x)$ would suggest a critical concentration near 0.35. This is in agreement with the reported value for x_c that lies between 0.35 [11] and 0.40 [13] depending if an upturn of $T_N(x)$ around x_c is considered or not.

The main result of this study is the abrupt change of the propagation vector from incommensurate to commensurate in $\text{CeRhIn}_{5-x}\text{Sn}_x$ in the vicinity of its magnetic quantum critical point where superconductivity is expected to occur. It is to be specified that, up to now, firmly established bulk superconductivity superconductivity is never reported at zero pressure for any given x but on applying 0.8 GPa starting from $x=0.16$ [14] or 0.6 GPa starting from $x=0.20$ [18]. These results suggest

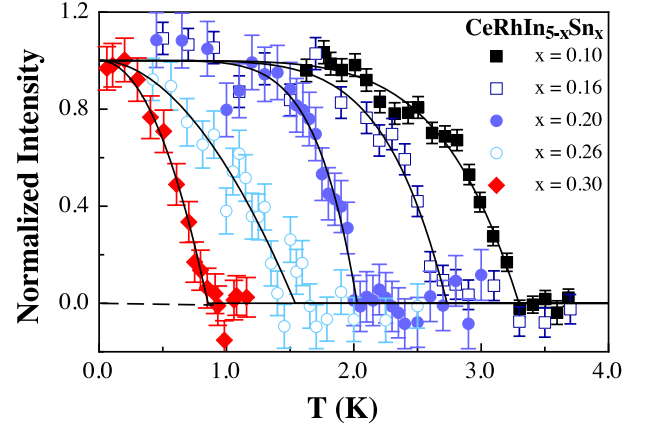


FIG. 4: Temperature dependence of the normalized magnetic intensities, for several x . Lines are phenomenological fits as explained in the text.

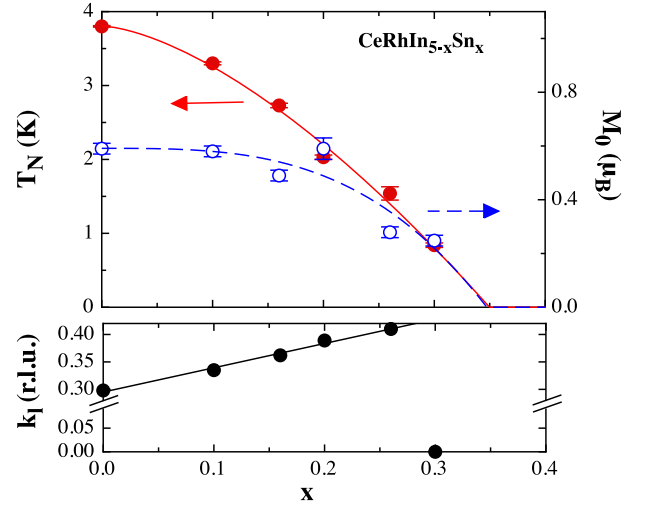


FIG. 5: Néel temperature, ordered magnetic moment and c -axis component of the propagation vector. Lines are guides for the eyes.

that further studies may evidence superconductivity at zero pressure in $\text{CeRhIn}_{5-x}\text{Sn}_x$ at higher x near x_c . On the other hand, when x increases, disorder increases and this may be detrimental to superconductivity. Having this in mind, one must nonetheless notice that similar changes of magnetic structure are already reported for several 1-1-5 related compounds for which superconductivity is firmly established.

A trend in the generic quantum critical (x, P, T) phase diagram of CeRhIn_5 related compounds is indeed the change from incommensurate to commensurate ordering associated with the appearance of superconductivity. This is observed for Ir and Co doped CeRhIn_5 for which ordering with $\mathbf{k}_G=(1/2, 1/2, 1/2)$ (G-type magnetic ordering) is reported either coexisting with or superseding the incommensurate ordering [19–22]. As concern CeRhIn_5 under pressure, NQR strongly suggests the

same G-type commensurate ordering above 1.7 GPa [7]. This is not confirmed by neutron scattering experiments that were performed up to this pressure. Nonetheless, a switching from $k_l \approx 0.30$ to $k_l \approx 0.40$ is found at lower pressure in relation with superconductivity [8, 9].

All these data suggest that commensurate antiferromagnetism with $\mathbf{k}_G=(1/2, 1/2, 1/2)$ is favorable for the formation of superconductivity in the quantum critical phase diagram of CeRhIn₅ related systems. Strikingly, we also observe here a commensurate ordering in CeRhIn_{5-x}Sn_x in the vicinity of x_c but with $\mathbf{k}_C=(1/2, 1/2, 0)$ instead of \mathbf{k}_G that would have been expected. This unachieved expectation was not only built upon the aforementioned literature but also upon the puzzling fact that the extrapolation of $k_l(x)$ to $k_l=1/2$ occurs for $x \approx x_c$. In addition, to our knowledge, a C-type magnetic ordering was never reported so far for rare-earth based 1-1-5 systems. This propagation vector is nonetheless the one of the magnetic order of the actinide based compound NpFeGa₅[23] and of several rare-earth based compounds related to the 1-1-5 ones by different sequences of atomic stacking [24].

As often pointed out, the Fermi surface topology is likely to play a key role for the determination of the magnetic ordering wavevector. This is specifically demonstrated for CeRhIn₅ by an *ab initio* calculation performed at $P=0$ that evidences a nesting of the Fermi surface for $k_l=0.375$, which is very close to the experimental value for the magnetic ordering wavevector \mathbf{k}_{IC} [25]. dHvA experiments are very powerful to track the modification of the Fermi surface as a function of P or x . A change of Fermi surface from localized character to itinerant character occurs under pressure in CeRhIn₅ at around 2.3 GPa where the superconducting transition temperature is maximum [26]. In a different way, Fermi surface reconstruction is also reported for Co substituted CeRhIn₅ when the magnetic structure switches from incommensurate to commensurate antiferromagnetism and when superconductivity occurs [27]. We can speculate that an abrupt modification of the Fermi surface occurs in CeRhIn_{5-x}Sn_x between $x=0.26$ and $x=0.30$ and this drives the switching of the propagation vector.

The systems reviewed above realize a case where T_N is higher than T_c and incommensurate magnetic ordering with $\mathbf{k}_{IC}=(1/2, 1/2, k_l)$ seems to be detrimental to superconductivity. The opposite situation ($T_N \leq T_c$) is also of great interest although experimental realization is scarce. Recently we have shown that in Ce_{0.95}Nd_{0.05}CoIn₅, magnetic ordering with the incommensurate propagation vector $\mathbf{k}_Q=(0.45, 0.45, 0.5)$ occurs [28]. This is the same propagation vector as the one of the field induced antiferromagnetic phase of CeCoIn₅ starting from the pure *d*-wave superconducting state. Here again Fermi surface topology is believed to play a key role. Since in both cases magnetic ordering occurs when superconductivity is established, it was suggested

that *d*-wave superconductivity with nodes in the nesting area favors such an incommensurate order with in-plane incommensurability.

Altogether these results suggest the possibility of collaborative effects between magnetism and superconductivity in the family of 1-1-5 compounds in relation with fine details of the Fermi surface. While the involved mechanisms are not necessarily the same for all these systems, magnetism and superconductivity can either compete or collaborate in 1-1-5 systems. These two opposite situations are likely to originate from the position of the nesting vector on the Fermi surface with respect to the superconducting order parameter nodes position.

In summary, we evidence a switching of magnetic propagation vector from incommensurate with $\mathbf{k}_{IC}=(1/2, 1/2, k_l)$ to commensurate with $\mathbf{k}_C=(1/2, 1/2, 0)$ in CeRhIn_{5-x}Sn_x in the proximity of its quantum critical point. Taking with caution the *P*-*x* analogy, this would correspond to a region of the phase diagram where superconductivity arises.

We acknowledge K. Mony for help in sample preparation. Cerium was provided by the Materials Preparation Center, Ames Laboratory, US DOE Basic Energy Sciences, Ames, IA, USA, available from: www.mpc.ameslab.gov.

-
- [1] Y. Uemura, Nature Materials 8 (2009) 253.
 - [2] J. L. Sarrao and J. D. Thompson: J. Phys. Soc. Jpn. **76** (2007) 051013 and references therein.
 - [3] G. Knebel, D. Aoki and J. Flouquet, C.R. Physique **12**, 542 (2011) and references therein.
 - [4] G. Knebel, D. Aoki, D. Braithwaite, B. Salce and J. Flouquet, Phys. Rev. B **74**, 020501 (2006).
 - [5] T. Park, F. Ronning, H. Q. Yuan, M. B. Salamon, R. Movshovich, J. L. Sarrao and J. D. Thompson, Nature **440** (2006) 65.
 - [6] M. Kenzelmann, Th. Strässle, C. Niedermayer, M. Sigrist, B. Padmanabhan, M. Zolliker, A. D. Bianchi, R. Movshovich, E. D. Bauer, J. L. Sarrao and J. D. Thompson, Science **321**, 1652-1654 (2008) and references therein.
 - [7] M. Yashima, H. Mukuda, Y. Kitaoka, H. Shishido, R. Settai and Y. Onuki, Phys. Rev. B **79** (2009) 214528 and references therein.
 - [8] S. Raymond, G. Knebel, D. Aoki and J. Flouquet, Phys. Rev. B **77**, 172502 (2008).
 - [9] N. Aso, K. Ishii, H. Yoshizawa, T. Fujiwara, Y. Uwatoko, G.-F. Chen, N.K. Sato and K. Miyake, J. Phys. Soc. Japan **78**, 073703 (2009).
 - [10] S. Raymond, E. Ressouche, G. Knebel, D. Aoki and J. Flouquet, J. Phys. Condens. Matter **19** (2007) 242204.
 - [11] E. Bauer, D. Mixson, F. Ronning, N. Hur, R. Movshovich, J. Thompson, J. Sarrao, M. Hundley, P. Tobash and S. Bobev: Physics B **378 – 80** (2006) 142.
 - [12] J. G. Donath, F. Steglich, E.D. Bauer, F. Ronning, J.L. Sarrao and P. Gegenwart, EPL **87**, 57011 (2009).
 - [13] J. G. Donath, P. Gegenwart, F. Steglich, E.D. Bauer and

- J.L. Sarrao, *Physica C* **460** – **462**, 661 (2007).
- [14] L. Mendonça, T. Park, V. Sidorov, M. Nicklas, E.M. Bittar, R. Lora-Serrano, E.N. Hering, S.M. Ramos, M.B. Fontes, E. Baggio-Saitovich, H. Lee, J.L. Sarrao, J. D. Thompson and P.G. Pagliuso, *Phys. Rev. Lett.* **101** (2008) 017005.
 - [15] P.C. Canfield and Z. Fisk, *Phil. Mag. B* **65**, 1117 (1992).
 - [16] G. Knebel, J. Buhot, D. Aoki, G. Lapertot, S. Raymond, E. Ressouche and J. Flouquet, *J. Phys. Soc. Jpn.* **80** (2011) SA001.
 - [17] J. Ruzs, P.M. Oppeneer, N.J. Curro, R.R. Urbano, B.-L. Young, S. Lebegue, P.G. Pagliuso, L.D. Pham, E.D. Bauer, J.L. Sarrao and Z. Fisk, *Phys. Rev. B* **77**, 245124 (2008).
 - [18] G. Knebel, unpublished.
 - [19] A.D. Christianson, A. Llobet, W. Bao, J.S. Gardner, I.P. Swaison, J.W. Lynn, J.-M. Mignot, K. Prokes, P.G. Pagliuso, N.O. Moreno, J. L. Sarrao, J.D. Thomson and A.H. Lacerda, *Phys. Rev. Lett.* **95**, 217002 (2005).
 - [20] S. Ohira-Kawamura, H. Shishido, A. Yoshida, R. Okazaki, H. Kawano-Furukawa, T. Shibauchi, H. Harima and Y. Matsuda, *Phys. Rev. B* **76**, 132507 (2007).
 - [21] M. Yokoyama, N. Oyama, H. Maitsuka, S. Oinuma, I. Kawasaki, K. Tenya, M. Matsuura, K. Hirota and T.J. Sato, *Phys. Rev. B* **77**, 224501 (2008).
 - [22] S. Ohira-Kawamura, H. Kawano-Furukawa, H. Shishido, R. Okazaki, T. Shibauchi, H. Harima and Y. Matsuda, *Phys. Status Solidi A* **206** 1076 (2009).
 - [23] F. Honda, N. Metoki, K. Kaneko, D. Aoki, Y. Homma, E. Yamamoto, Y. Shiokawa, Y. Onuki, E. Colineau, N. Bernhoeft and G. Lander, *Physica B* **359** – **361**, 1147 (2005).
 - [24] P. Čermák, P. Javorský, M. Kratochvílová, Karel Pajskr, Milan Klicpera, Bachir Ouladdiaf, Marie-Hélène Lemée-Cailleau, Juan Rodriguez-Carvajal and Martin Boehm, *Phys. Rev. B* **89** (2014) 184409 and references therein.
 - [25] T. Bjorkman, R. Lizarraga, F. Bultmark, O. Eriksson, J.M. Wills, A. Bergman, P.H. Andersson and L. Nordstrom, *Phys. Rev. B* **81**, 094433 (2010).
 - [26] H. Shishido, R. Settai, H. Harima and Y. Onuki, *J. Phys. Soc. Japan* **74**, 1103 (2005).
 - [27] S. K. Goh, J. Paglione, M. Sutherland, E.C.T. O’Farell, C. Bergemann, T.A. Sayles and M.B. Maple, *Phys. Rev. Lett.* **101**, 056402 (2008).
 - [28] S. Raymond, S.M. Ramos, D. Aoki, G. Knebel, V.P. Mineev and G. Lapertot, *J. Phys. Soc. Japan* **83**, 013707 (2014).